

## Research Article

Wei Yang, Dapeng Xu, Tao Chen, Jianli Wang, and Jian Chen\*

# Microstructure and photocatalytic performance of micro arc oxidation coatings after heat treatment

<https://doi.org/10.1515/secm-2020-0002>

Received Nov 08, 2017; accepted Feb 27, 2019

**Abstract:** A V-doped titania catalyst was synthesized on titanium substrate by micro-arc oxidation and then it was carried out by heat treatment in nitrogen atmosphere. The surface characteristics of the synthesized titania coatings were investigated by SEM, EDS, XPS and XRD. The synthesized  $\text{TiO}_2$  coating doped with V (in form of  $\text{V}_2\text{O}_3$  and  $\text{V}_2\text{O}_5$ ) showed a large amount of “cellular” bulges with more microscopic defects. The anatase phase of the  $\text{TiO}_2$  coatings after heat treatment tended to be transformed into rutile phase. As a result, the corrosion resistance and photocatalytic performance of  $\text{TiO}_2$  coating doped with V after heat treatment had been enhanced.

**Keywords:** Micro arc oxidation; Heat treatment; Microstructure; Photocatalysis; Corrosion

## 1 Introduction

In recent years, photocatalyst materials have attracted significant interest among researchers for application in environmental remediation due to their outstanding photocatalytic performance towards organic pollutants degradation [1–3]. It is well known that metal oxide photocatalysis is a very promising approach to solve the pollution problem. Among various metal oxide, titanium oxide ( $\text{TiO}_2$ ) has become one of the most popular photocatalysis for its chemically inert and photocatalytically stable, and so on. The preparation of photocatalytic  $\text{TiO}_2$  coatings on the substrates has been the main research direction cur-

rently. A number of commonly surface techniques have been developed to synthesize titanium dioxide, such as sol-gel, chemical vapor deposition, cold spray, spray pyrolysis, and anodizing [4, 5]. Micro arc oxidation (MAO) is one of the most promising and environmentally friendly technology to prepare  $\text{TiO}_2$  coatings, which could be carried out by ultrasonic catalysis, light-ound and light-lectric combined catalysis. It has recently gained much attention as useful photocatalysis for its simple manufacturing process, high growth rate and adhesion, porous microstructure, excellent anti vibration performance [6–9]. Since the band gap energy ( $E_g$ ) of titania is relatively wide, considerable efforts have been extended to broaden the absorption edge of  $\text{TiO}_2$  toward the visible part of the spectrum in the last three decades, and so it is expected to be a new method for the preparation of high performance  $\text{TiO}_2$  photocatalytic coating. The  $\text{TiO}_2$  coatings doped with metallic or nonmetallic elements (such as Ag, V, W, B, N and S) to enhance the photocatalytic properties have been reported by some references [10–13]. Furthermore, heat treatment is another method for improving the photocatalytic properties of the coatings and also beneficial for increasing the coating adhesion strength, which is used in  $\text{TiO}_2$  thin film or powder [14–16]. However, heat treatment to influence the microstructure and photocatalytic performance of  $\text{TiO}_2$  coatings has been little reported.

In this paper, the  $\text{TiO}_2$  coatings formed by MAO were prepared on pure titanium in the electrolytes with or without  $\text{NaVO}_3$  addition. Then, the obtained coatings were carried out by heat treatment. Finally, the microstructure and photocatalytic performance of the  $\text{TiO}_2$  coatings with or without V doping before and after heat treatment had been comparatively studied. Meanwhile, the mechanical, electrochemical and photocatalytic performances of  $\text{TiO}_2$  coatings were also systematically studied.

**\*Corresponding Author: Jian Chen:** School of Materials Science and Chemical Engineering, Xi'an Technological University, Xi'an 710032, China; Email: chenjian@xatu.edu.cn; Tel. +86 029 86173324; Fax: +86 029 86173324

**Wei Yang, Dapeng Xu, Jianli Wang:** School of Materials Science and Chemical Engineering, Xi'an Technological University, Xi'an 710032, China

**Tao Chen:** Jiangsu Provincial Key Laboratory of Advanced Robotics & Collaborative Innovation Center of Suzhou Nano Science and Technology, Soochow University, Suzhou 215123, China

## 2 Experimental

### 2.1 Preparation of MAO coatings

Pure titanium ( $\Phi 16\text{ mm} \times 5\text{ mm}$ ) was mechanically polished to an average surface roughness of  $R_a \approx 28.6\text{ nm}$ , followed by ultrasonic cleaning in acetone for 10 min. To fabricate  $\text{TiO}_2$  ceramic coatings, the constant voltage mode was selected and 450 V was predefined. The MAO parameters were as follows: frequency 500 Hz, duty cycle 6% and time 5 min. The solution temperature was kept below  $35^\circ\text{C}$  during the MAO process. Three electrolytes, 10 g/L  $\text{Na}_2\text{SiO}_3$ , 20 g/L  $\text{Na}_2\text{SiO}_3$ , 20 g/L  $\text{Na}_2\text{SiO}_3 + \text{NaVO}_3$ , were used for the MAO deposition. As a result, the three  $\text{TiO}_2$  coatings with the thickness of about  $8\text{ }\mu\text{m}$  were prepared. In the further text, we would use the terms “MAO-1, MAO-2, MAO-3” to denote the three  $\text{TiO}_2$  coatings. Then the three obtained  $\text{TiO}_2$  coatings were carried out by heat treatment using tube furnace (KSY, Beijing Kewei Instrument Co. Ltd. Yongxing, China), using “MAO-1+HT, MAO-2+HT, MAO-3+HT” to denote the three  $\text{TiO}_2$  coatings after heat treatment. Due to the relatively small size, the three samples wrapped with tin foil were loaded in porcelain boats during the heat treatment process. The annealing temperature for heat treatment were set at  $400^\circ\text{C}$  in  $\text{N}_2$ , at which the specimens were kept for 60 min. In the final step, the samples were left in the furnace to cool naturally.

### 2.2 Coating characterization

Field-emission scanning electron microscopy with energy dispersive X-ray spectrometer (EDS) (FE-SEM, S-4800, Hitachi, Japan) were performed for morphological characterization of the  $\text{TiO}_2$  coatings. X-ray diffraction meter with  $\text{Cu K}\alpha$  radiation was used to study the phases of the obtained  $\text{TiO}_2$  coatings. The x-ray generator was operated at 40 kV and 40 mA. X-ray photoelectron spectroscopy (XPS, Axis ultraDLD, Japan) with Al (mono)  $\text{K}\alpha$  irradiation at pass energy of 160 eV was used to characterize the chemical bonds of the coatings. The binding energies were referenced to the C 1s line at 285.0 eV.

### 2.3 Property testing

The corrosion resistance of the coatings was tested by the electrochemical system (PGSTAT302, OTL, Holland) under room temperature using electrochemical potentiodynamic polarization in 5 wt.% NaCl solution. During the process of electrochemical test, a three electrode cell with the coated

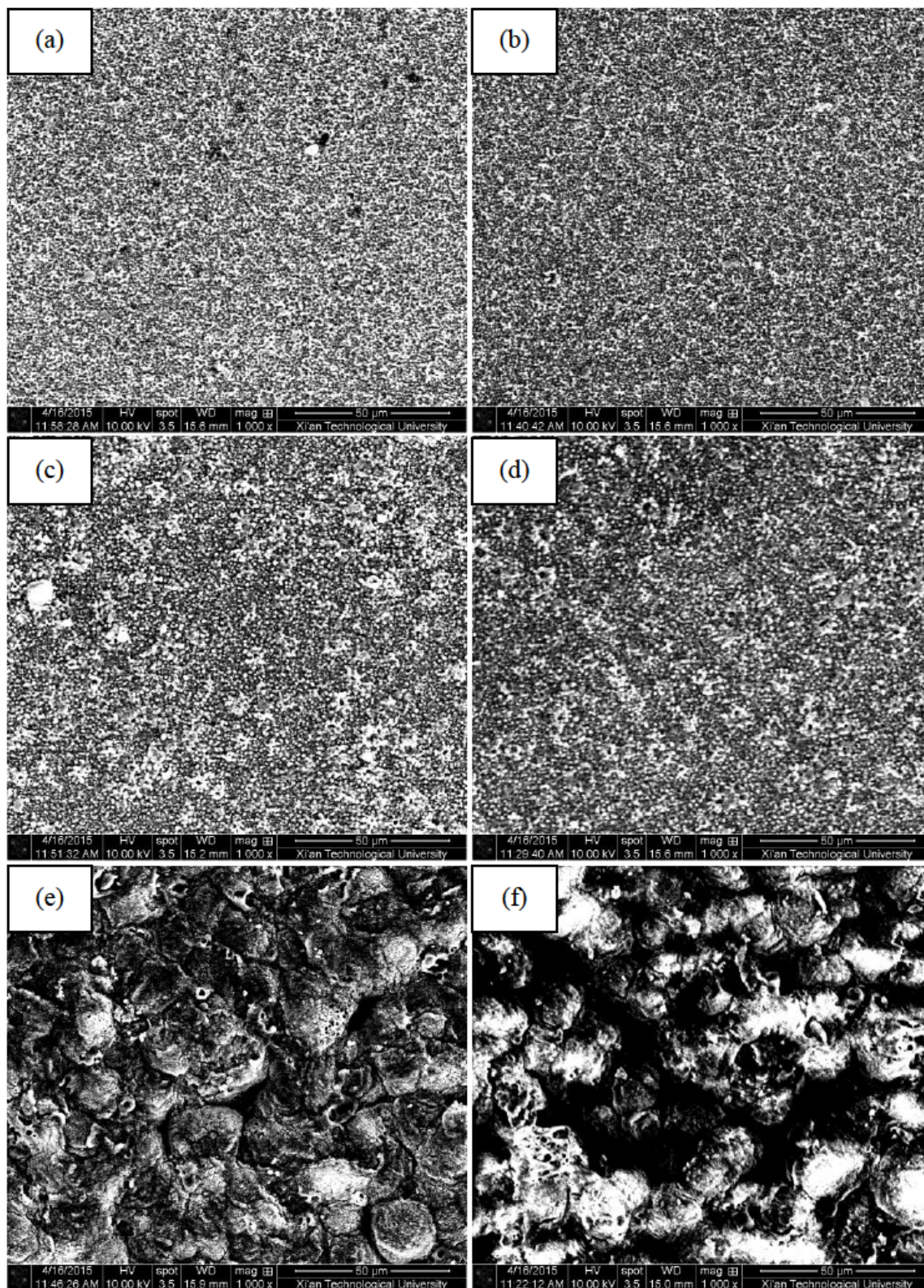
specimens as working electrode, the platinum sheet as auxiliary electrode, the saturated calomel electrode as the reference electrode was used. The working electrode was covered with a holder with a circular window having a surface area of  $0.785\text{ cm}^2$  and was exposed to the electrolytic solution. Before each measurement, the open circuit potential (OCP) of samples was monitored for 5 min to stabilize the surface condition. The scanning speed was 1 mV/s. A 64 bit system -zview software was used to fit and calculate the characterization parameters of electrochemical corrosion. The photocatalytic activities of the prepared samples were measured by determining the degradation of methylene blue (MB) solution, and a 8 W ultraviolet lamp was used as the light source of simulated sunlight. The distance between the samples and the lamp was 5 cm. The concentration of the MB solution was 8 mg/L and the test sample was fully immersed in 10 ml of MB solution. The decomposition rates of MB were monitored by measuring the absorbance of MB solution at 664 nm using a UV 723 spectrophotometer periodically every 1 h for a total time of 5 h. The coated samples were tested for the average value.

## 3 Results and discussion

### 3.1 Coating characteristics

Figure 1 shows the surface morphologies of  $\text{TiO}_2$  coatings prepared in three different electrolytes on pure Ti substrates. It was found that the surface morphologies of  $\text{TiO}_2$  coatings prepared in 10 g/L or 20 g/L  $\text{Na}_2\text{SiO}_3$  solutions were compact and smooth, which was not clearly changed before and after heat treatment under  $400^\circ\text{C}$  for 1 h. After adding 5 g/L  $\text{NaVO}_3$  into 20 g/L  $\text{Na}_2\text{SiO}_3$  base solution, energy applied to the sample under the same electrical parameter output conditions had been enhanced and micro arc phenomenon could be strengthened during the MAO process. So high energy resulted in more spattering of molten droplets and more holes observed in the ceramic coating. As a result, some “cellular” bulge and micropores were found on this  $\text{TiO}_2$  coating. Compared with the  $\text{TiO}_2$  coating prepared in 10 g/L or 20 g/L  $\text{Na}_2\text{SiO}_3$  solutions, the  $\text{TiO}_2$  coating prepared in 20 g/L  $\text{Na}_2\text{SiO}_3 + 5\text{ g/L NaVO}_3$  solutions was more coarse obviously. Furthermore, the surface defects on the  $\text{TiO}_2$  coating doped with V were increased after heat treatment. These “defects” microstructure might be beneficial for increasing the adsorption of organic matter on the coating surface and improving its

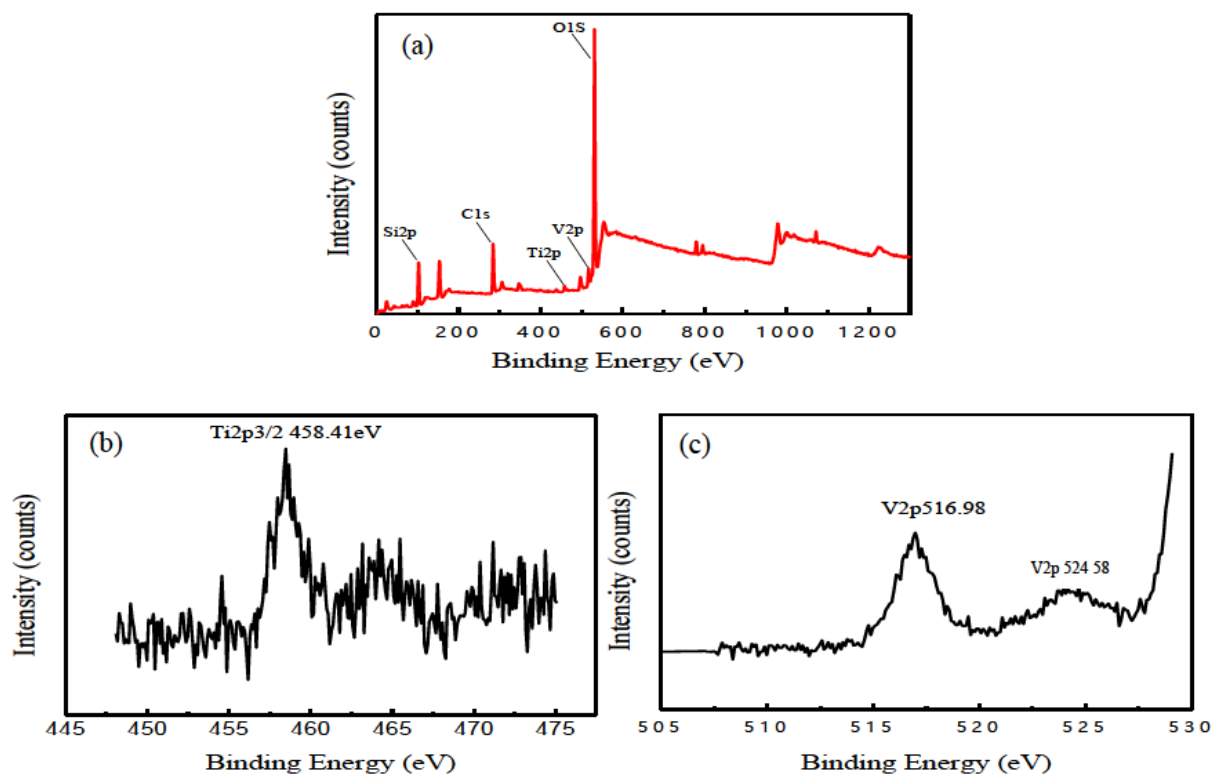




**Figure 1:** Surface morphologies of MAO coatings before and after heat treatment (a) MAO-1, (b) MAO-1+HT, (c) MAO-2, (d) MAO-2+HT, (e) MAO-3, (f) MAO-3+HT

**Table 1:** EDS results of MAO coatings prepared on Ti substrates before and after heat treatment

Coatings	O	Ti	Si	Na	C	V
MAO-1	71.56	16.05	11.91	0.39	0.09	
MAO-2	71.66	10.67	17.26	0.34	0.07	
MAO-3	65.81	10.11	20.01	1.12	0.12	1.29
MAO-1+HT	71.22	16.47	11.80	0.50		
MAO-2+HT	70.79	11.16	17.56	0.43	0.06	
MAO-3+HT	64.55	10.15	20.53	1.26	0.06	1.59

**Figure 2:** (a) XPS survey spectra, (b) typical  $Ti2p_{3/2}$  and (c)  $V2p$  high-resolution XPS spectrum of MAO coating doped with V on Ti substrate after heat treatment

photocatalytic performance due to the increase of surface area.

The EDS analysis of the  $TiO_2$  coatings in three different electrolytes was shown in Table 1. It was found that the elementary compositions of the  $TiO_2$  coatings formed in the same electrolyte had no obvious change before and after heat treatment. The content of Si element was increased significantly, as the  $TiO_2$  coating was prepared in an increased concentration of  $Na_2SiO_3$ . Meanwhile, the content of Ti element significantly reduced and O content was not significantly changed. So, it was obtained that Si element from the electrolyte was strongly involved in the formation process of  $TiO_2$  coating. The introduction of V into the base  $Na_2SiO_3$  solution resulted in a sharp micro arc discharge

phenomenon. As a result, V and Si elements from the electrolyte strongly participated in the formation process of  $TiO_2$  coating, which resulted in the decreased content of O and Ti elements in the coating. So it was obtained that the degree of solute ions participating in the  $TiO_2$  coatings could be affected by each other.

In order to study the elemental composition of the  $TiO_2$  coating doped with V after heat treatment, the XPS analysis has been employed. The XPS survey spectra of the prepared coating is shown in Figure 2 (a). It was noted that the dominant elements were O, Ti, Si, V and C. The high concentration of C was commonly in the surface XPS scan, which was attributable to environmental contamination. The concentration of Ti and O elements were 11.28



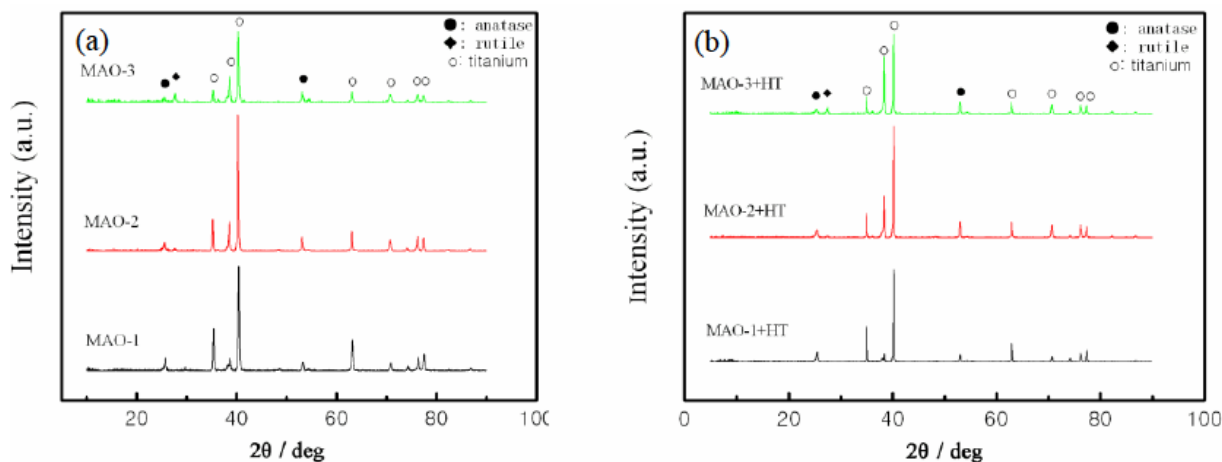


**Figure 3:** XRD patterns for three MAO coatings formed onto Ti substrates, (a) before heat treatment, (b) after heat treatment

**Table 2:** Ratio of anatase and rutile phases of MAO coated Ti substrates before and after heat treatment

Coatings	Ratio of anatase and rutile
MAO-1	Only anatase
MAO-2	Only anatase
MAO-3	10.28
MAO-1+HT	8.45
MAO-2+HT	1.81
MAO-3+HT	0.85

at.% and 63.67 at.%, respectively. The V2p peak of the TiO<sub>2</sub> coating had been found and the atomic percentage of the V element in this coating was 1.85 at.%, which indicated that the V element from the solution had been doped into the TiO<sub>2</sub> coating. Furthermore, a large amount of Si element (about 18.36 at.%) from the base solution had been obviously detected, which illustrated that the solute element had been strongly involved in the formation process of TiO<sub>2</sub> coatings. This was consistent with some literatures [17, 18]. The Ti2p<sub>3/2</sub> peak of TiO<sub>2</sub> coating was shown on Figure 2 (b), and the Ti2p<sub>3/2</sub> peak of 558.41 eV indicated the existence of TiO<sub>2</sub>. So it could be obtained that the titanium oxide was formed in this TiO<sub>2</sub> coating. The V2p peak of TiO<sub>2</sub> coating was shown on Figure 2 (c). The V2p<sub>3/2</sub> peak of 516.98 eV and V2p<sub>1/2</sub> peak of 524.58 eV corresponded to V<sub>2</sub>O<sub>3</sub> and V<sub>2</sub>O<sub>5</sub>, respectively. Therefore, it was confirmed by XPS analysis that V element from the solution was incorporated into the oxide film through the electrochemical oxidation process. According to M.R. Bayati *et al.* [19], the absorption edge of the TiO<sub>2</sub> coating doped with V (V<sub>2</sub>O<sub>5</sub>) shifted toward the visible wavelengths and the photocatalytic performance of this composited TiO<sub>2</sub> coating could

be enhanced. Thus it could be speculated that the photocatalytic performance of the obtained TiO<sub>2</sub> coating doped with V might be changed compared with the TiO<sub>2</sub> coating without V doping [20].

The XRD patterns of the oxidized samples prepared by different MAO technology are presented in Figure 3. The proportion of anatase and rutile phase of different TiO<sub>2</sub> coatings is shown in Table 2. XRD analysis revealed that the surfaces of the coated samples were covered by Ti and TiO<sub>2</sub>. The appearance of Ti peaks on the XRD patterns was most likely due to the penetration of the X-rays beyond the TiO<sub>2</sub> coating. The TiO<sub>2</sub> coating prepared in 10 g/L Na<sub>2</sub>SiO<sub>3</sub> solution included only anatase TiO<sub>2</sub> before and after heat treatment. The crystalline phase of the pure TiO<sub>2</sub> film is anatase, because it is very difficult for the metastable anatase phase to transform to thermodynamically stable rutile phase due to less heat produced by mild spark discharge on the surface of anode for a low conductivity of the solution. Xiang *et al.* [10] also reported that TiO<sub>2</sub> film was mainly composed of anatase generated during MAO process. Furthermore, it was found that the crystalline phase of the pure TiO<sub>2</sub> film after heat treatment was still composed of anatase phase. When the concentration of Na<sub>2</sub>SiO<sub>3</sub> was increased to 20 g/L, the TiO<sub>2</sub> coatings included anatase TiO<sub>2</sub> and rutile TiO<sub>2</sub>, and the proportion of anatase phase and rutile phase was 10.28, which was due to a violent discharge on anodic surface and resulted in the transformation of crystalline phase from metastable anatase phase to thermodynamically stable rutile phase. The proportion of anatase phase and rutile phase of this TiO<sub>2</sub> coating after heat treatment decreased to 8.45, implying that the metastable anatase phase further transformed into thermodynamically stable rutile phase. With the addition of NaVO<sub>3</sub> into 20 g/L Na<sub>2</sub>SiO<sub>3</sub> solution, the TiO<sub>2</sub> coat-

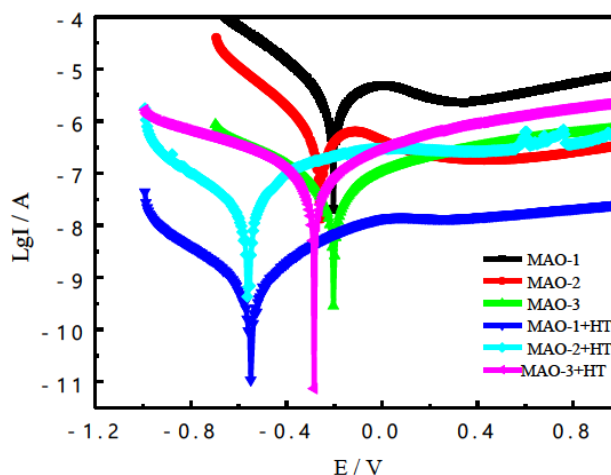
**Table 3:** Electrochemical parameters obtained from the polarization curves of Figure 4

Coatings	Corrosion current density (A/cm <sup>2</sup> )	Corrosion potential (V)
MAO-1	$6.037 \times 10^{-8}$	-0.205
MAO-2	$8.998 \times 10^{-8}$	-0.2593
MAO-3	$9.31 \times 10^{-8}$	-0.2061
MAO-1+HT	$1.492 \times 10^{-9}$	-0.5506
MAO-2+HT	$5.922 \times 10^{-9}$	-0.5577
MAO-3+HT	$4.894 \times 10^{-8}$	-0.284

ings also included anatase TiO<sub>2</sub> and rutile TiO<sub>2</sub> before and after heat treatment, and the proportion of anatase phase and rutile phase was 1.81 and 0.85, respectively. Compared with the TiO<sub>2</sub> coatings without V doping, the proportion of anatase and rutile phase of the TiO<sub>2</sub> coatings with V doping significantly decreased due to the change of micro arc discharge characteristics and the function of V element in the coatings [20]. It was also believed that anatase phase of the TiO<sub>2</sub> coatings prepared in 20 g/L Na<sub>2</sub>SiO<sub>3</sub> electrolytes with or without NaVO<sub>3</sub> addition tended to be transformed to rutile phase after heat treatment. As a result, the TiO<sub>2</sub> coatings with different proportion of anatase and rutile phase could present different properties, especially the photocatalytic performance.

### 3.2 Corrosion resistance

In order to study the corrosion resistance of MAO treated Ti substrate when it serves as photocatalytic material, an in corrosion test is employed and the potentiodynamic polarization curves are used to evaluate the corrosion resistance [21, 22]. The polarization curves of the coated pure Ti substrates in the 3.5 wt.% NaCl solution are shown in Figure 4. Corrosion potential and corrosion current density obtained from Figure 5 by Tafel analysis are shown in Table 3. Based on these electrochemical parameters, it was known that the corrosion current density and corrosion potential of the MAO coated samples after heat treatment all slightly decreased compared with the MAO coated samples before heat treatment, which indicated that the corrosion resistance of the MAO coated samples after heat treatment got better and the corrosion tendency had been intensified [23]. It was known that the metastable anatase phase could be transformed into thermodynamically stable rutile phase of the MAO coating on Ti substrate after heat treatment, which resulted in the enhanced corrosion resistance. However, adding 5 g/L NaVO<sub>3</sub> into 20 g/L solution, the obtained TiO<sub>2</sub> coating showed the worst corrosion resistance due to the increasing micro “defects” and

**Figure 4:** Polarization curves of three MAO coatings before and after heat treatment

the potential difference between Ti and V elements, which might result in the galvanic corrosion. Besides, the MAO coating doped with V element resulted in the decreased content of O and Ti elements in the coating, which was not also helpful for the improvement of its corrosion resistance. In general, the weakened corrosion resistance of the MAO coating doped with V was due to surface morphologies with some “defects” (pore size), galvanic corrosion between Ti and V elements, and change of Ti and O (Composition of titanium oxide) element content.

### 3.3 Photocatalytic activity

The photocatalytic activity of the TiO<sub>2</sub> coatings on pure Ti before and after heat treatment versus illumination time is shown in Figure 5 (a) and (b). It was found that the photodegradation rate of methylene blue gradually increased along with the illumination time for all the TiO<sub>2</sub> coatings before and after heat treatment, and the photodegradation rate increased fast first and then the increasing speed tended to be slow. The photodegradation rate of methylene

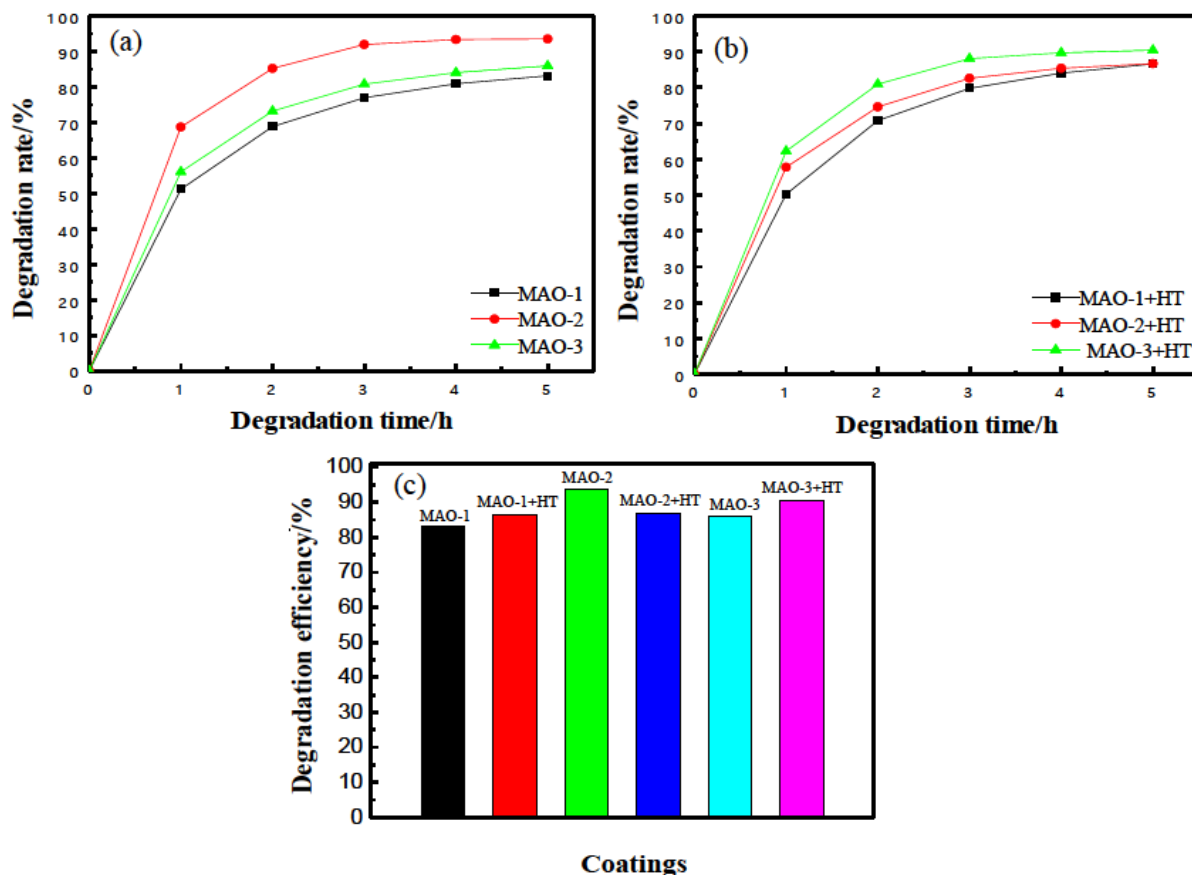


**Figure 5:** Photocatalytic activity of three MAO coatings (a) before heat treatment, (b) after heat treatment, (c) catalytic effect of MAO coatings for 5 h

blue for the  $\text{TiO}_2$  coatings prepared in 20 g/L  $\text{Na}_2\text{SiO}_3$  solution with or without V doping was higher than the  $\text{TiO}_2$  coating prepared in 10 g/L  $\text{Na}_2\text{SiO}_3$  solution before heat treatment, which could be mainly attributed to the mixed phase and the transfer of photo-generated electron from rutile to anatase. In addition, metal oxides with more structure defects on surface are able to substantially ionosorb oxygen to improve the photocatalytic activity [24]. However, the photocatalytic activity of the  $\text{TiO}_2$  coating doped with V was lower than the  $\text{TiO}_2$  coating prepared in 20 g/L  $\text{Na}_2\text{SiO}_3$  solution, which might attribute to the proportion of anatase phase and rutile phase. The  $\text{TiO}_2$  coating doped with V presented the highest photodegradation rate among the three  $\text{TiO}_2$  coatings after heat treatment due to comprehensive function of the proportion of the mixed phase and the formation of structural defects. The photodegradation efficiencies of the  $\text{TiO}_2$  coatings before and after heat treatment were shown in Figure 5 (c). Compared with the  $\text{TiO}_2$  coating doped with V, the photodegradation efficiency of this  $\text{TiO}_2$  coating after heat treatment had been enhanced. It was believed that the “defects” mi-

crostructure, doping V into the coating and the decreasing proportion of anatase and rutile phase resulted in the increasing adsorption of organic matter on the coating surface and enhancing the photocatalytic activity. However, the photodegradation efficiency of the  $\text{TiO}_2$  coating prepared in 20 g/L  $\text{Na}_2\text{SiO}_3$  solution had been deteriorated after heat treatment. In short, the  $\text{TiO}_2$  coating prepared in 20 g/L  $\text{Na}_2\text{SiO}_3$  solution before heat treatment had the best photodegradation efficiency among the all  $\text{TiO}_2$  coatings, which was determined by a appropriate proportion of anatase and rutile phase to accelerate photo-generated electron transferring from rutile to anatase.

## 4 Conclusion

1. The  $\text{TiO}_2$  coatings prepared in the base electrolyte were smooth and compact, and their surface morphologies changed little after heat treatment. Adding  $\text{NaVO}_3$  into the base electrolyte, some “cellular” bulges were found on the coating and heat treat-

ment resulted in an increase of micro “defects” and a poor corrosion resistance for this coating.

2. The coating prepared in 10g/L Na<sub>2</sub>SiO<sub>3</sub> electrolyte was only composed of anatase phase, which was not changed before and after heat treatment. The anatase phase and rutile phase were all found in the two coatings prepared in the 20g/L Na<sub>2</sub>SiO<sub>3</sub> electrolyte or 20g/L Na<sub>2</sub>SiO<sub>3</sub> + 5g/L NaVO<sub>3</sub> electrolytes. The ratios of anatase phase and rutile phase were all decreased after heat treatment.
3. The TiO<sub>2</sub> coating prepared in 20 g/L Na<sub>2</sub>SiO<sub>3</sub> solution showed the best photodegradation efficiency before heat treatment for a appropriate proportion of anatase and rutile phase, but it could be deteriorated after heat treatment. The TiO<sub>2</sub> coating doped with V presented the best photodegradation efficiency among the three coatings after heat treatment.

**Acknowledgement:** The authors gratefully acknowledge the financial support of the Key research and development plan of shaanxi province- Industrial project (Grant No. 2018GY127).

## References

- [1] Y.L. Song, P.H. Shao, J.Y. Tian, W.X. Shi, S.S. Gao, J.Y. Qi, X.J. Yan, F.Y. Cui, One-step hydrothermal synthesis of ZnO hollow nanospheres uniformly grown on graphene for enhanced photocatalytic performance, *Ceram. Int.* 42 (2016) 2074-2078.
- [2] X.W. Lu, X.Z. Li, J.C. Qian, N.M. Miao, C. Yao, Z.G. Chen, Synthesis and characterization of CeO<sub>2</sub>/TiO<sub>2</sub> nanotube arrays and enhanced photocatalytic oxidative desulfurization performance, *J. Alloys Compd.* 661 (2016) 363-371.
- [3] Q.Z. Wang, D.H. Jiao, Y. Bai, J.B. Zhong, L.C. Zhao, X. Yong, J.H. Tong, J.Z. Li, Immobilized Heteropolyacids with zeolite (MCM-41) to enhance photocatalytic performance of BiOBr, *Mater. Lett.* 161 (2015) 267-270.
- [4] J.L. Jia, D. Li, J.F. Wan, X.J. Yu, Characterization and mechanism analysis of graphite/C-doped TiO<sub>2</sub> composite for enhanced photocatalytic performance, *J. Ind. And Eng. Chem.* 33 (2016) 162-169.
- [5] Z.M. Wu, X. Tong, P.T. Sheng, W.L. Li, X.H. Yin, J.M. Zou, Q.Y. Cai, Fabrication of high-performance CuInSe<sub>2</sub> nanocrystals-modified TiO<sub>2</sub> NTs for photocatalytic degradation applications, *Appl. Surf. Sci.* 351 (2015) 309-315.
- [6] Q. Luo, Q.Z. Cai, X.W. Li, Z.H. Pan, Y.J. Li, X.D. Chen, Q.S. Yan, Preparation and characterization of ZrO<sub>2</sub>/TiO<sub>2</sub> composite photocatalytic film by micro-arc oxidation, *T. Nonferr. Metal. Soc.* 23 (2013) 2945-2950.
- [7] K.R. Wu, C.H. Hung, C.W. Yeh, J.K. Wu, Microporous TiO<sub>2</sub>-WO<sub>3</sub>/TiO<sub>2</sub> films with visible-light photocatalytic activity synthesized by micro arc oxidation and DC magnetron sputtering, *Appl. Surf. Sci.* 263 (2012) 688-695.
- [8] S.C. Di, Y.P. Guo, H.W. Lv, J. Yu, Z.W. Li, Microstructure and properties of rare earth CeO<sub>2</sub>-doped TiO<sub>2</sub> nanostructured composite coatings through micro-arc oxidation, *Ceram. Int.* 41 (2015) 6178-6186.
- [9] W.P. Li, M.Q. Tang, L.Q. Zhu, H.C. Liu, Formation of microarc oxidation coatings on magnesium alloy with photocatalytic performance, *Appl. Surf. Sci.* 258 (2012) 10017-10021.
- [10] N. Xiang, R.G. Song, B. Xiang, H. Li, Z.X. Wang, C. Wang, A study on photocatalytic activity of micro-arc oxidation TiO<sub>2</sub> films and Ag+/MAO-TiO<sub>2</sub> composite films, *Appl. Surf. Sci.* 347 (2015) 454-460.
- [11] M.R. Bayati, A.Z. Moshfegh, F. Golestani-Fard, On the photocatalytic activity of the sulfur doped titania nano-porous films derived via micro-arc oxidation, *Appl. Catal. A- Gen.* 389 (2010) 60-67.
- [12] J.H. Lee, J.I. Youn, Y.J. Kim, I.K. Kim, K.W. Jang, H.J. Oh, Photocatalytic characteristics of boron and nitrogen doped titania film synthesized by micro-arc oxidation, *Ceram. Int.* 41 (2015) 11899-11907.
- [13] M.R. Bayati, A.Z. Moshfegh, F. Golestani-Fard, In situ growth of vanadia-titania nano/micro-porous layers with enhanced photocatalytic performance by micro-arc oxidation, *Electrochim. Acta* 55 (2010) 3093-3102.
- [14] Y. Lu, K. Matsuzaka, L. Hao, Y. Hirakawa, H. Yoshida, F.S. Pan, Photocatalytic activity of TiO<sub>2</sub>/Ti composite coatings fabricated by mechanical coating technique and subsequent heat oxidation, *Mater. Sci. Semicond. Process.* 16 (2013) 1949-1956.
- [15] B. Rahmati, E. Zalnezhad, Ahmed A.D. Sarhan, Z. Kamiab, B. Nasiri Tabrizi, W.A.B.W. Abas, Enhancing the adhesion strength of tantalum oxide ceramic thin film coating on biomedical Ti-6Al-4V alloy by thermal surface treatment, *Ceram. Int.* 41 (2015) 13055-13063.
- [16] S. Sado, T. Ueda, K. Ueda, T. Narushima, Formation of TiO<sub>2</sub> layers on commercially pure Ti and Ti-Mo and Ti-Nb alloys by two-step thermal oxidation and their photocatalytic activity, *Appl. Surf. Sci.* 357 (2015) 2198-2205.
- [17] W. Yang, J.L. Wang, D.P. Xu, J.H. Li, T. Chen, Characterization and formation mechanism of grey micro-arc oxidation coatings on magnesium alloy, *Surf. Coat. Technol.* 283 (2015) 281-285.
- [18] X. Ma, S.J. Zhu, L.G. Wang, C.X. Ji, C.X. Ren, S.K. Guan, Synthesis and properties of a bio-composite coating formed on magnesium alloy by one-step method of micro-arc oxidation, *J. Alloys Compd.* 590 (2014) 247-253.
- [19] M.R. Bayatia, A.Z. Moshfegh, F. Golestani-Fard, Synthesis of narrow band gap (V<sub>2</sub>O<sub>5</sub>)<sub>x</sub>-(TiO<sub>2</sub>)<sub>1-x</sub> nano-structured layers via micro arc oxidation, *Appl. Surf. Sci.* 256 (2010) 2903-2909.
- [20] F.Z. Ren, H.Y. Li, Y.X. Wang, J.J. Yang, Enhanced photocatalytic oxidation of propylene over V-doped TiO<sub>2</sub> photocatalyst: Reaction mechanism between V<sup>5+</sup> and single-electron-trapped oxygen vacancy, *Appl. Catal., B* 176-177 (2015) 160-172.
- [21] S. Durdu, A. Aytaç, M. Usta, Characterization and corrosion behavior of ceramic coating on magnesium by micro-arc oxidation, *J. Alloys Compd.* 509 (2011) 8601-8606.
- [22] X.Y. Lu, X.G. Feng, Y. Zuo, C.B. Zheng, S. Lu, L. Xu, Evaluation of the micro-arc oxidation treatment effect on the protective performance of a Mg-rich epoxy coating on AZ91D magnesium alloy, *Surf. Coat. Technol.* 270 (2015) 227-235.
- [23] C.J. Wang, B.L. Jiang, M. Liu, Y.F. Ge, Corrosion characterization of micro-arc oxidation composite electrophoretic coating on



AZ31B magnesium alloy, J. Alloys Compd. 621 (2015) 53-61.

- [24] A. Sclafani, J.M. Herrmann, Comparison of the Photoelectronic and Photocatalytic Activities of Various Anatase and Rutile Forms of Titania in Pure Liquid Organic Phases and in Aqueous Solutions, J. Phys. Chem. 100 (1996) 13655-13661.